Available online at BCREC Website: http://bcrec.undip.ac.id

Bulletin of Chemical Reaction Engineering & Catalysis, 12 (3), 2017, 415-429

Research Article

Low Temperature Selective Catalytic Reduction (SCR) of NOx Emissions by Mn-doped Cu/Al_2O_3 Catalysts

Deepak Yadav[1], Ashish R. Kavaiya[1], Devendra Mohan[2], Ram Prasad[1,*]

[1]Department of Chemical Engineering & Technology, Indian Institute of Technology (Banaras Hindu University), Varanasi, 221 005, India
[2]Department of Civil Engineering, Indian Institute of Technology (Banaras Hindu University), Varanasi, 221 005, India

Received: 5th January 2017; Revised: 20th May 2017; Accepted: 20th May 2017; Available online: 27th October 2017; Published regularly: December 2017

Abstract

The 15 mol% Cu/Al_2O_3 catalysts with different Mn doping (0.5, 1.0, 1.5, mol%) were prepared using PEG-300 surfactant following evaporation-induced self-assembly (EISA) method. Calcination of precursors were performed in flowing air conditions at 500 ºC. The catalysts were characterized by X-ray Diffraction (XRD), X-ray Photoelectron Spectroscopy (XPS), Scanning Electron Microscope Energy Dispersive X-Ray (SEM-EDX), Fourier Transform Infra Red (FTIR), and N_2 physisorption. The catalysts activities were evaluated for H_2 assisted LPG-SCR of NO in a packed bed tubular flow reactor with 200 mg catalyst under the following conditions: 500 ppm NO, 8 % O_2, 1000 ppm LPG, 1 % H_2 in Ar with total flow rate of 100 mL/min. Characterization of the catalysts revealed that surface area of 45.6-50.3 m^2/g, narrow pore size distribution (1-2 nm), nano-size crystallites, Cu^{2+} and Mn^{2+} phases were principal active components. Hydrogen enhanced significantly selective reduction of NO to N_2 with LPG over 1.0 mol % Mn-Cu/Al_2O_3 giving 95.56 % NO reduction at 150 ºC. It was proposed that the synergistic interaction between H_2 and LPG substantially widened the NO reduction temperature window and a considerable increase in both activity and selectivity. Negligible loss of catalyst activity was observed for the 50 h of stream on run experiment at 150 ºC. The narrow pore size distribution, thermal stability of the catalyst and optimum Mn doping ensures good dispersion of Cu and Mn over Al_2O_3 that improved NO reduction in H_2-LPG SCR system.

Keywords: Mn-doped Cu/Al_2O_3; Selective Catalytic Reduction; SCR; NOx; H_2-LPG; de-NOx

How to Cite: Yadav, D., Kavaiya, A.R., Mohan, D., Prasad, R. (2017). Low Temperature Selective Catalytic Reduction (SCR) of NOx Emissions by Mn-doped Cu/Al_2O_3 Catalysts. *Bulletin of Chemical Reaction Engineering & Catalysis*, 12 (3): 415-429 (doi:10.9767/bcrec.12.3.895.415-429)

Permalink/DOI: https://doi.org/10.9767/bcrec.12.3.895.415-429

1. Introduction

Multiple-growth of vehicular count and increasing industrialization emit toxic nitrogen oxides (NOx) as primary pollutants directly into atmosphere [1]. The NOx photo-chemically reacts with atmospheric constituents and produces more lethal secondary pollutants viz. acid rain, ozone, smog, etc. [2]. In addition, NOx also cause global warming, and climate change. To prevent adversarial effects on health and environment, legislations require continuous strictness through upgrading pollution abatement techniques. Both light-duty and heavy-duty vehicles emission need more modern clean de-NOx exhaust technologies to improve air quality [3]. Therefore, NOx abatement has become a signifi-

* Corresponding Author.
E-mail: rprasad.che@itbhu.ac.in (Prasad, R.)
Telp.: +91-9415268192

cant concern and a focused approach is needed to amend or develop the technologies to reduce NOx emission. In the last few decades, many de-NOx studies have been focused on exhaust gas recirculation (EGR), catalytic decomposition of NOx, lean-burn NOx traps (LNT), and selective catalytic reduction (SCR) of NOx. Among several NOx control techniques SCR of NOx with reductants such as NH_3, urea, hydrocarbon, or H_2-hydrocarbon are the most effective way [4-6]. For automotive NOx emission control applications, it is necessary to develop a highly active, selective and robust SCR catalyst. The catalyst should selectively convert NOx in presence of a reductant into environmentally benign N_2 molecules. Consequently, great efforts have been made to develop SCR catalysts with large specific surface area and pore diameter Al_2O_3 support [1,4].

Catalyst is the key to SCR technology and its performance directly affects the abatement of NOx emissions. Different types of SCR catalysts are reported in the literature such as platinum group metal (Pt, Pd, Rh, etc.), precious metal (Ag/Al_2O_3, $Au-Ag/Al_2O_3$) and transition metals (V_2O_5-WO_3/TiO_2, Cu-ZSM-5, Fe-ZSM-5, etc.) [7-12]. PGM catalysts are highly active but they are costly, low abundance and vulnerable to further price increases with increasing demand. Therefore, the need to explore PGM free catalyst with transition metals is of global research prominence. Transition metal oxide-based catalysts are inexpensive, resistant to poisoning and higher active surface area compared to noble metal oxides [13]. Consequently, transition metal oxides have been intensively studied to discover more economical and effective catalysts for low-temperature SCR of NOx.

A great number of scientific publications relate to cheaper catalysts than PGM catalysts for SCR processes have been reported. The MnO_x, NiO_x, CuO_x, CeO_x, and mixed metal oxides have been studied as promising cheap and low temperature SCR catalysts. The commercial catalysts V_2O_5-WO_3/TiO_2 and V_2O_5-WO_3 (MO_3)$/TiO_2$ were widely used as NH_3-SCR in stationary engines exhaust, encounter difficulties such as ammonia slip, air heater fouling, ammonium sulfate deposition and being hazardous not a good choice for vehicular engines. Cu-ZSM-5 and Fe-ZSM-5 are highly active and stable at high temperatures but hydrothermally unstable make them not viable for commercial applications [14].

Transition metal oxides mixed with noble metals to reduce the cost have also been testified, such as: Pt-Cu/Mg-Al, Pt-K/$MgAl_2O_4$, Ru/Mg-Co-Al, etc. Such catalysts showed better NO mitigation at higher temperatures (>250 °C) than transition metal catalysts [15]. Cu-based catalysts are considered to be promising that might become potential candidates for the replacement of V_2O_5-WO_3/TiO_2 for their low cost, low toxicity and high activity at low temperatures [16]. CuO_x/ZrO_2, CuO_x/WO_x-ZrO_2, $CuO/Ti_{0.95}Ce_{0.05}O_2$, and zeolite-supported copper catalysts (Cu-BEA, Cu-SSZ-13, Cu/SAPO-34 and so on) show excellent low-temperature NH_3-SCR activities [17]. Various reductants like NH_3, urea, hydrocarbons (HC), H_2 assisted HC/NH_3, ethanol, hydrogen, CO, alcohols, amines, etc. are studied to reduce NOx in presence of catalyst [18].

Several reactions occur in an NH_3-SCR system that reduces NOx to nitrogen, can be illustrated as Equations (1-3) [19]. The dominant reaction is represented by Equation (1).

$$4NO + 4NH_3 + O_2 \rightarrow 4N_2 + 6H_2O \quad (1)$$

Competing, non-selective reactions with oxygen can produce secondary emissions or may unproductively consume ammonia. One such non-selective reaction is the complete oxidation of ammonia, shown by Equation (2).

$$4NH_3 + 5O_2 \rightarrow 4NO + 6H_2O \quad (2)$$

Also, side reactions may lead to undesirable products such as N_2O, as represented by Equation (3).

$$5NO + 4NH_3 + 3O_2 \rightarrow 4N_2O + 6H_2O \quad (3)$$

The SCR of NOx reaction using hydrocarbon like LPG (~72 % propane) and H_2-assisted HC can be illustrated as Equations (4, 5).

$$2NO + C_3H_8 + 4O_2 \rightarrow N_2 + 3CO_2 + 4H_2O \quad (4)$$

$$2NO + C_3H_8 + H_2 + 5.5O_2 \rightarrow N_2 + 3CO_2 + 5H_2O \quad (5)$$

There are dominantly two reductants were used for diesel vehicular exhaust; first is Urea-SCR and the second one is HC-SCR. Recently, commercial SCR systems employed in heavy-duty trucks and also in a few light-duty lean-burn vehicles are based on aqueous 32.5 % urea solution (AdBlue), which hydrolyzes to release ammonia in the hot exhaust gas system [20]. The released ammonia reduces the NOx on the SCR catalyst to form nitrogen and water. The major drawbacks with such SCR system are NH_3-slip, ash odor, air heaters plugging and formation of harmful by-products.

The side reactions of NH_3 oxidation over catalyst above 240 °C with O_2 concentration above 5 % produce N_2O and NO_2 [21]. The side reactions compete with the SCR reaction for NH_3 and hence, the NO conversion is reduced. Further, urea only hydrolyses to ammonia in hot exhaust gas above 200 °C, it is not possible to inject urea during at lower temperature and consequently NOx emissions reduction drops. Also, extra cost of storage in the vehicles is objectionable factor. These key facts enforced researchers to find out alternate reductant for low temperature NO-SCR.

The potential use of LPG (~72 % C_3H_8) as reducing agent in the SCR of NOx is a better alternative to the other reductants as it leads to a strong decrease in the Gibbs free energy values of NO reduction to N_2 than other reductants (Table 1) [22]. In addition, LPG offers better system integration, as it is readily obtainable and is used as a fuel for many utilities and encouraged for use in motor vehicles.

Therefore, an alternative strategy for meeting NOx emission regulations that does not exhibit the difficulties of the aforementioned methods is HC-SCR [23]. The better selectivity of NO reduction to N_2 in case of H_2-LPG ensures less susceptibility to side reactions [24]. Further, recent invention shows that addition of small amounts of hydrogen to the diesel engine exhaust can significantly improve the performance [25].

Manganese doped catalyst significantly improves the low temperature SCR activity [26]. The key factors are identified to be (1) high specific surface area and surface acidity; (2) additional surface adsorbed oxygen on the catalyst surface (3) well dispersion of MnO_x [27]. The MnO_x showed the redox property of lattice oxygen [28]. It has been found that Mn doping in a catalyst lowers down the temperature for NOx SCR [29-31]. Among all, Mn-based catalysts have acknowledged for high de-NOx potential at low temperatures [32]. However, improvement in NOx conversions, broadening of temperature window and time on stream patterns still need to be improved.

There is no work reported on Mn doped Cu/Al_2O_3 catalyst using H_2-LPG reductant in the open literature for de-NOx. Thus, in the present study Mn doped Cu based catalysts were comparatively investigated and concluded that they are low cost, possess good NO-SCR activity at low temperature and high selectivity to N_2 with H_2-LPG reductant.

2. Materials and Method

2.1 Catalyst preparation

Three Mn doped Cu/Al_2O_3 catalysts with different concentrations were prepared along with Cu/Al_2O_3 catalyst following the EISA procedure suggested by Li *et al.* [1]. In the synthesis of Copper-alumina catalysts 8.3 mL polyethylene glycol (PEG-300) was dissolved in 150 mL of ethanol at room temperature termed as solution-1. In a container, 12.0 mL of 69 % nitric acid, 3.75 g citric acid anhydrous, 15.30 g (15 mmol) of aluminium iso-propoxide, 15 mol% of copper nitrate trihydrate and requisite amount of $Mn(NO_3)_2$ were added in the above solution-1 with vigorous stirring for 10 h. The final solution was dried overnight at 110 °C in an oven, followed by in-situ calcination in flowing air at 500 °C for 5 h. The calcined samples were crushed and sieved to pass a 100 mesh for activity testing. All the chemicals used in the catalyst preparation are of AR grade. For the simplicity in general consideration, the catalysts were name as: Cu/Al_2O_3 as Cat-A, 0.5 % $Mn\text{-}Cu/Al_2O_3$ Cat-B, 1.0 % $Mn\text{-}Cu/Al_2O_3$ Cat-C and 1.5 % $Mn\text{-}Cu/Al_2O_3$ as Cat-D.

2.2 Catalytic activity measurement

The NO-SCR activity tests were studied in a tubular quartz reactor over 200 mg catalyst diluted with 1 mL Al_2O_3 bed kept over quartz wool under the following reaction conditions: 500 ppm NO, 8 % O_2, 1000 ppm NH_3, 1000 ppm LPG, 1 % H_2 in Ar with total flow rate of 100 mL/ min. Gases were fed from pressurized cylinders. The experimental data were recorded under steady state conditions. The space velocity was 30000 $mL.g^{-1}.h^{-1}$. The reaction temperatures were varied from ambient to 450 °C. Three different reductants (H_2, LPG, and NH_3) were used separately under the same experimental conditions. In addition, H_2 assisted LPG (H_2-LPG) reduction was also investigated. The temperature of reaction was monitored with the help of K-type thermocouple inserted in the thermo-well of the reactor in contact with catalyst bed. The reaction temperature

Table 1. Gibbs free energy at 500 K for reduction of NO in the presence of various reductants

Reductant	H_2	CO	NH_3	CH_4	C_3H_8	C_4H_{10}
$-\Delta G_r$ (kJ/mol)	605.8	646.3	367.5	543.9	603.1	557.7

and rate of heating was controlled with help of micro-processor based temperature controller. The flow of gas mixture entering the reactor was free from moisture and CO_2 via passing them through CaO and KOH pellet trap. The flow rates of different gases were monitored with the help of digital gas flow meters. The inlet and outlet NOx concentrations were determined by Ecophysics CLD 62 chemiluminescence NO/NOx analyzer. The concentration of propane and CO_2 as well as the N_2 was measured by two online gas chromatographs using FID and TCD detectors (Nucon 5765) and porapack q-column with methanizer and molecular sieve 5A respectively.

The conversion of NO at any instant was calculated on the basis of values of the concentration of NO in the feed, NO conversion (X_{NO}) was calculated as follows: and product stream by the following Equation (6):

$$X_{NO}(\%) = \left(1 - \frac{[NO_{out}]}{[NO_{in}]}\right) x100 \quad (6)$$

The conversion of main LPG constituents, C_3H_8, C_4H_{10} and i-C_4H_{10} were calculated on the basis of values of their concentrations in the feed and product using the following Equations (7-9):

$$X_{C_3H_8} = 1 - \left[\frac{A_{C_3H_{8_{out}}}}{A_{C_3H_{8in}}}\right] \quad (7)$$

$$X_{C_4H_{10}} = 1 - \left[\frac{A_{C_4H_{10_{out}}}}{A_{C_4H_{10in}}}\right] \quad (8)$$

$$X_{i-C_4H_{10}} = 1 - \left[\frac{A_{i-C_4H_{10_{out}}}}{A_{i-C_4H_{10in}}}\right] \quad (9)$$

where, the subscripts "in" and "out" indicate the inlet and outlet concentrations respectively at steady state. The change in concentration of C_3H_8, C_4H_{10} and i-C_4H_{10} is due to redox reactions at any instant is proportional to their respective areas of chromatograms [A_{C3H8}], [A_{C4H10}], and [$A_{i\text{-}C4H10}$].

The N_2 selectivity can be written in terms of concentration of N_2 and other by-products (NO_2 and N_2O) by Equation (10):

$$N_2\ selectivity(\%) = 100x\left\{\frac{[N_2]}{[NO_2]+[N_2O]+[N_2]}\right\} \quad (10)$$

2.3 Catalyst Characterization

X-ray diffractograms were measured on Rigaku Ultima IV X-ray diffractometer (Germany) using the Cu Kα radiation at 40 kV and 40 mA for phase identification. The spectra were recorded between 20 and 80° (2θ). The mean crystallite size (d) of the catalyst was calculated from the line broadening of the most intense reflection using the Scherrer's formula in Equation (11).

$$d = \frac{0.89\lambda}{\beta\cos\theta} \quad (11)$$

where d is the mean crystallite diameter, 0.89 is the Scherrer constant, λ is X-ray wavelength (Cu Kα radiation) = 1.54056 Å, and β is effective line width of the observed X-ray reflection, calculated by the expression $\beta^2=B^2-b^2$; where B is full width half maximum (FWHM) and b is instrumental broadening determined through the FWHM of the X-ray reflection at 2θ of crystalline SiO_2.

X-ray photoelectron spectroscopy (XPS) was used to monitor the surface compositions and chemical states of the constituent elements and performed on an Amicus Spectrometer equipped with Mg Kα X-ray radiation. For typical analysis, the source was operated at a voltage of 15 kV and current of 12 mA. The binding energy scale was calibrated by setting the main C 1s line of adventitious impurities at 284.7 eV, giving an uncertainty in peak positions of ~ 0.2 eV. Scanning electron micrographs (SEM) and SEM-EDX were recorded on Zeiss EVO 18 scanning electron microscope (SEM) instrument. An accelerating voltage of 15 kV and magnification of 1000X was applied. Energy-dispersive X-ray analysis (EDX) was collected on a JEOL JEM 2010 microscope operating at 200 kV equipped with a PGT Imix PC system. Specific surface area (SSA) measurements were performed using Micromeritics ASAP 2020 analyzer by physical adsorption of N_2 at the temperature of liquid nitrogen (-196 °C), using the BET method in the standard pressure range of 0.05-0.30 P/P_0. Fourier transform infrared spectroscopy (FTIR) of the prepared catalyst was recorded in the range of 400-4000 cm^{-1} on Shimadzu 8400 FTIR spectrometer with KBr pellets at room temperature.

3. Results and Discussion

3.1 Catalyst Characterization

3.1.1 X-Ray diffraction

X-ray diffraction (XRD) studies were carried out to identify the crystalline phases of the catalyst samples. The powder XRD patterns of the crystalline nature of Cat-A and Mn doped catalysts (Cat-B, Cat-C and Cat-D) were confirmed by collecting intensity data over a 2θ = 20-80° is depicted in the Figure 1. The characteristics reflections of Cat-A as well as three different concentration of Mn doped catalysts showed single diffraction peak at 2θ = 22.72°, which could be attributed to a single phase crystalline structure of Al_2O_3 (JCPDS#310026). The diffraction peaks of Cu and Mn could not be observed for Mn doped catalysts, which clearly indicated that the Cu and Mn ions were well-dispersed over Al_2O_3 support. The increase in the amount of Mn doping in Cu/Al_2O_3, the intensities of Al_2O_3 diffraction peaks decreased significantly [33].

3.1.2 XPS analysis

X-ray photoelectron spectra (XPS) were recorded to investigate elemental composition and the oxidation state of the catalysts sample near the surface. Figure 2 (a-d) displays the XPS spectra in the Cu-2p, Mn-2p, Al-2p and O-

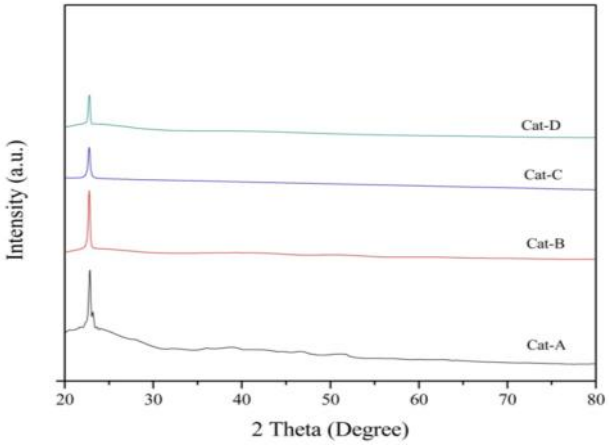

Figure 1. XRD pattern of Cu/Al_2O_3 and Mn-doped Cu/Al_2O_3 catalyst

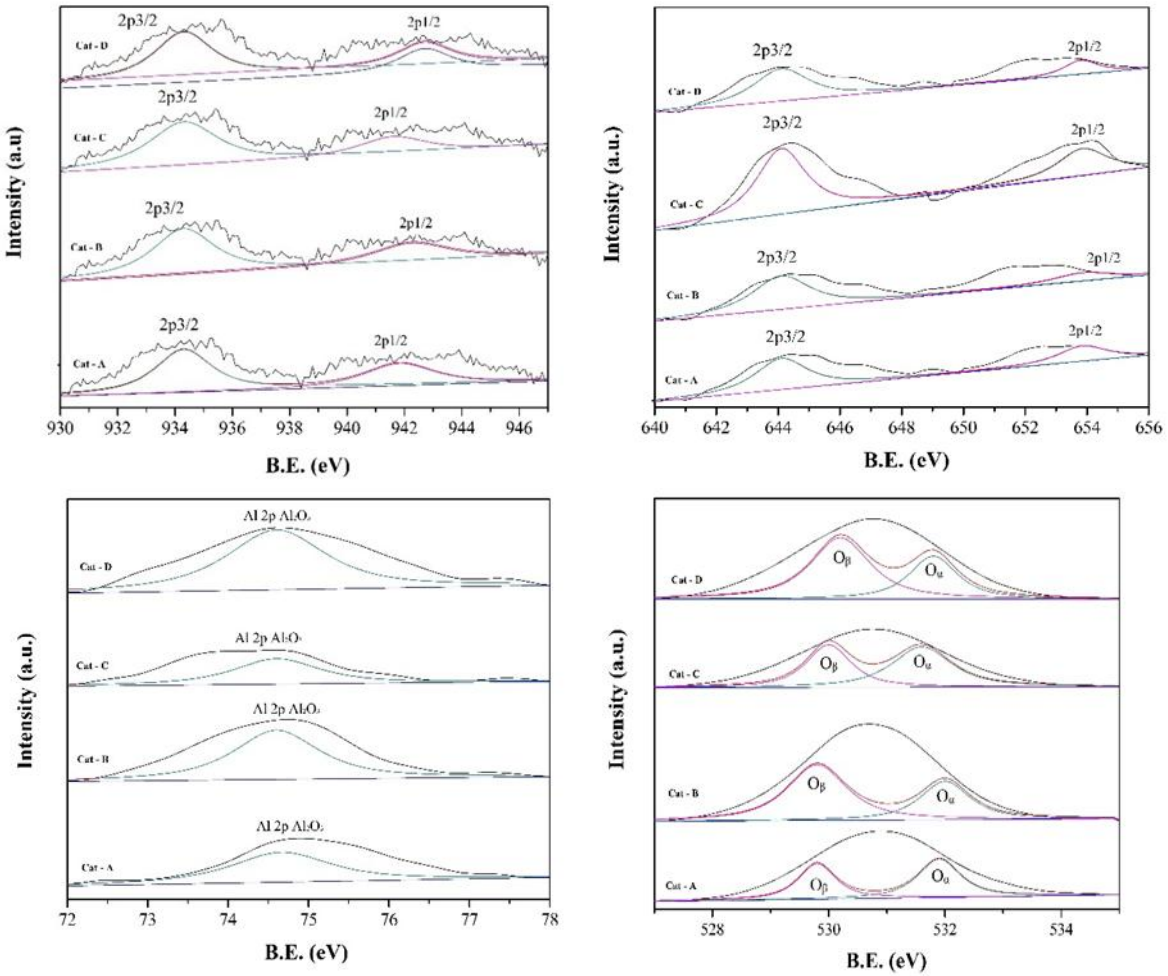

Figure 2. XPS peak fitting of (a) Cu, (b) Mn, (c) Al and (d) O for Cat-A, B, C and D.

1s regions. The corresponding results as shown in Figure 2(a) reveals that the only Cu, Mn, Al and O elements are present in the catalyst. Using a Gaussian fitting method, it was observed that the Cu2p emission spectra was well fitted with two spin-orbit doublets, implying both Cu^{+} and Cu^{2+} in the catalyst sample. The peaks fitted at the binding energies of 934.3 and 948.4 eV attributed to Cu-$2p_{3/2}$ and Cu-$2p_{1/2}$ configurations [34,35]. Although, it can be proposed that highest Cu^{+}/Cu^{2+} are preferable for the reduction of NO.

The XPS spectra in the Mn-2p region are presented in Figure 2(b). The observed binding energies 644.8 eV, and 653.85 eV are associated with the presence of Mn^{2+} and Mn^{3+} respectively in their respective samples [36,37]. BE of Al-2p is shown at 74.6 eV revealed Al^{3+} oxidation state as shown in Figure 2(c). The binding energies of O-1s are displayed in Figure 2(d). Generally, there are two different types of oxygen in the catalysts with binding energy 532.2 eV and 534.1 eV, which could be predictable as chemisorbed oxygen and lattice oxygen, respectively [38]. The presence of chemisorbed oxygen is small as compared to lattice oxygen in Cat-C. One of noticeable fact is that the amount of oxygen is less in Cat-C as compared to all three catalysts due to absence of lattice oxygen which creates oxygen vacancies for reduction reactions.

3.1.3 Scanning Electron Micrographs (SEM)

SEM analysis was done to study the surface morphology of the catalysts. Figure 3 shows the SEM micrographs of Cat-A and Mn doped Cat-B, Cat-C and Cat-D. It can be visualized that all the catalysts have particles of irregular shapes and sizes. The shape of Cat-A was the agglomerated bulk particles of the largest size. The size of the particles of Cat-C (Figure 3c) was the smallest as well as it possessed open texture pores in comparison to the other catalysts. Other catalyst samples were appeared to be agglomerated whereas Cat-C was well dispersed separated particles of size in the range

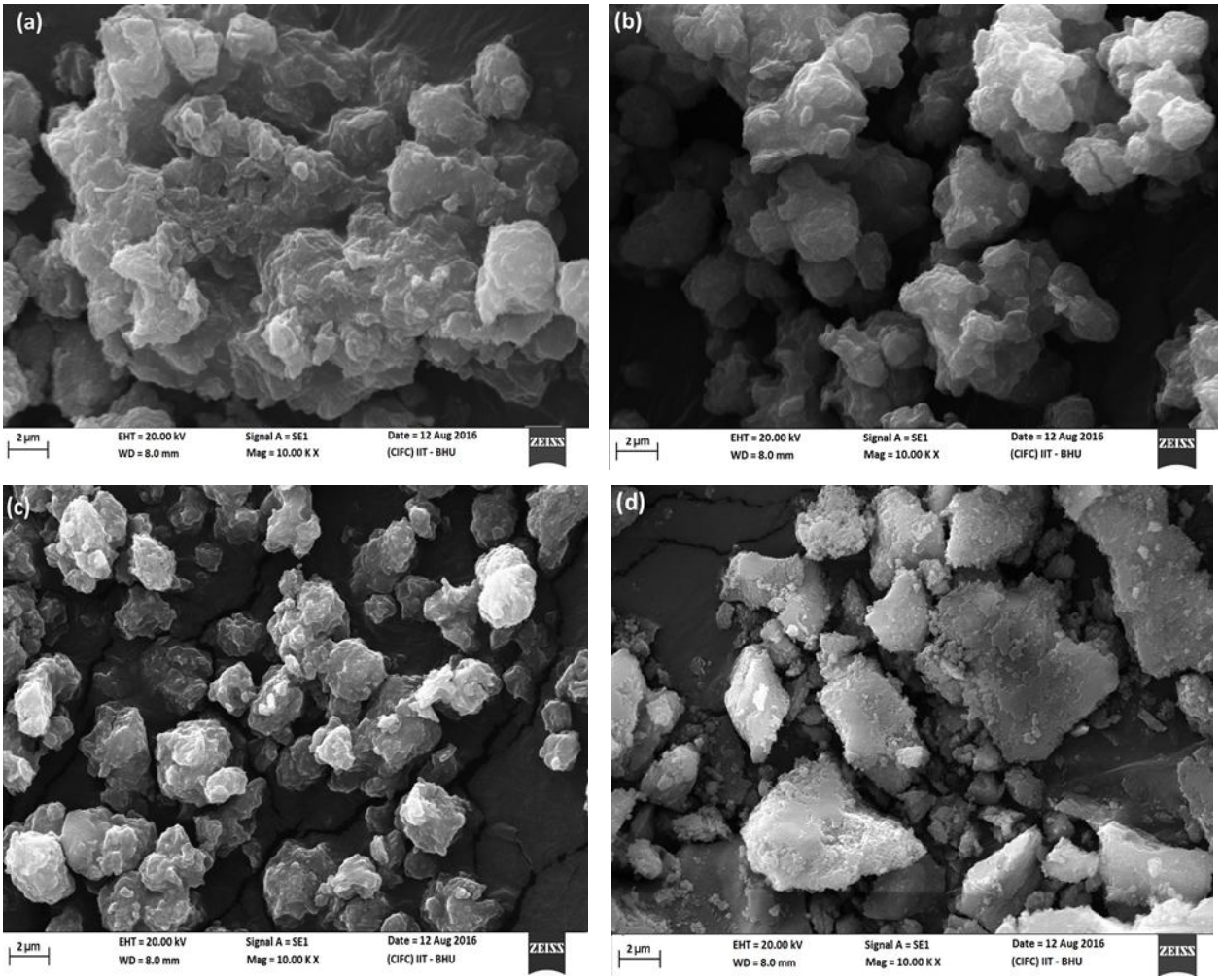

Figure 3. SEM micrographs of (a) Cat-A, (b) Cat-B, (c) Cat-C, and (d) Cat-D.

of 2.07-3.32 µm. Since the particles of Cat-C were the smallest and well dispersed it decreases the resistance of internal mass-transport of reactants and products. Beyond the optimum content of Mn (1.0 %) in the catalyst, different structures of agglomerated particles of larger size were formed. Hence, the optimum composition of Mn was 1.0 % in Cat-C for low temperature SCR of NO.

3.1.4 Energy-dispersive X-ray Analysis (EDX)

The elemental composition of the Cat-C microspheres was first examined by energy dispersive X-ray (EDX) measurements. Energy dispersive X-ray (EDX) results from different regions of micrographs depicts that all the samples were pure due to presence of Cu, Mn, Al, and O peaks. No other element present in the spectra as shown in Figure 4.

EDX spectrum details of all three catalysts samples with their respective weight and atomic % is given in Table 2. Elemental mapping analysis and corresponding EDX-mapping images clearly elucidate the confirm the formation of respective atomic content in their relevant structure.

SEM-EDX confirmed the presence of Cu, Mn, Al, and O elements present in the precursors used in the preparation of the catalysts. Cu and Mn dispersions on the Al_2O_3 surface was found to be sufficient, with some agglomerates appearing for the catalysts.

3.1.5 Fourier Transform Infrared Spectroscopy (FTIR)

The term 'Fresh catalyst' meant freshly prepared Cat-C (unused) and 'used catalyst' was after 50 h of run on stream for H_2-LPG-SCR of NO. FTIR of fresh and used catalysts were recorded in the range of 500-4000 cm^{-1} on Shimadzu 8400 FTIR spectrometer with KBr pellets at room temperature in terms of transmittance. The absorption spectra of the two catalysts during the course of H_2-LPG-SCR reac-

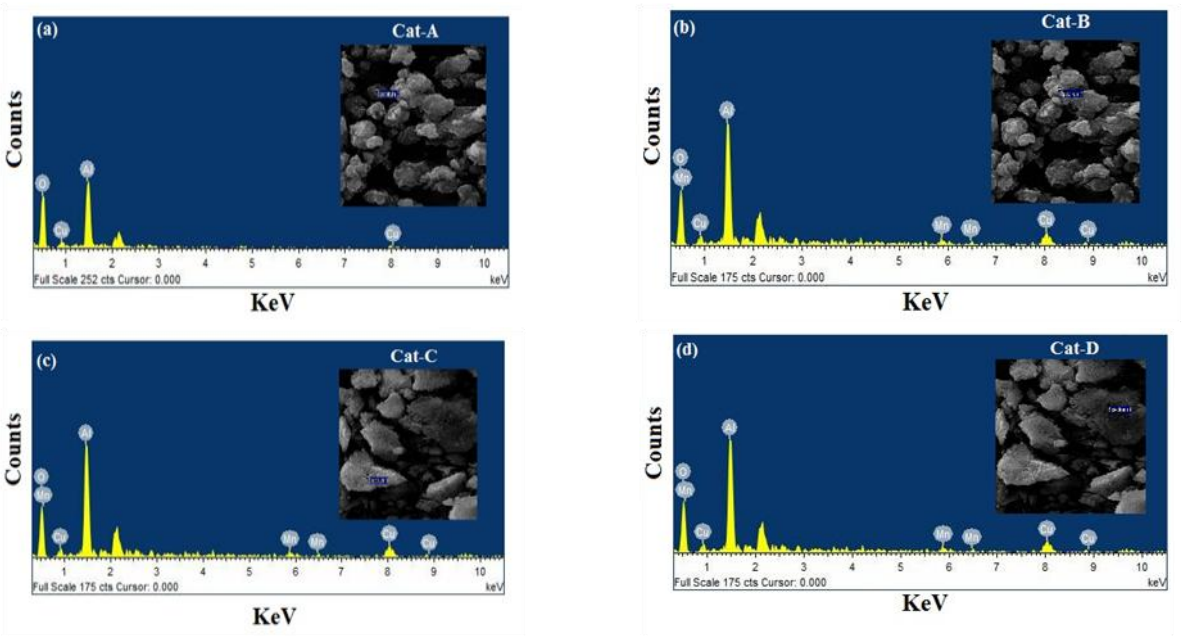

Figure 4. EDX spectrum and elemental micrographs of (a) Cat-A, (b) Cat-B, (c) Cat-C, and (d) Cat-D

Table 2. Weight % and atomic % (EDX elemental data) for all four catalysts

	Cat-A		Cat-B		Cat-C		Cat-D	
Element	Weight%	Atomic%	Weight%	Atomic%	Weight%	Atomic%	Weight%	Atomic%
O K	43.76	61.67	49.58	59.92	37.14	50.41	45.08	50.50
Al K	40.96	23.04	29.81	21.06	44.65	29.84	34.72	30.32
Cu K	15.28	15.29	19.63	18.23	17.03	18.3	18.56	16.53
Mn K	-	-	0.98	0.79	1.18	1.45	1.63	1.65
Total	100.00		100.00		100.00		100.00	

tion over the Cat-C surface is showed in Figure 5 the stretching vibrations of metal-oxygen bond.

The bands at 1700-1300 cm^{-1} are associated to the N–C stretching modes, which are caused by the different doping level [39]. The bands at 1200-1600 cm^{-1} were slightly stronger, indicating that a few of the Lewis acid sites were occupied by bridging nitrate species [40]. The NO conversion changed from 95.56 % to 90.7 % at 150 °C with accelerated ageing after 50h. As we can see from Figure 5 and Table 3, C≡N stretch i.e. nirile group is missing due to reductant (H_2-LPG), responsible for better NO reduction at the surface of Cat-C. FTIR transmission spectra of the catalysts are comparison shown in Table 3.

3.1.6 BET surface area measurement

The specific surface area and pore size distribution were determined by BET and BJH methods with low temperature adsorption on all four catalysts. The BET surface area, pore volume and pore diameter of respective catalysts were tabulated in Table 4. The BET surface area data indicates that the BET surface area of Cat-A, Cat-B, and Cat-D are smaller than Cat-C (50.29 m^2g^{-1}), because of the high dispersion shown in SEM micrographs. The Cat-C catalyst has the maximum BET surface area and pore volume due to their high pore diameter compared to rest three catalyst. The BET surface area of the Cat-D was 46.85 m^2/g due to the formation of a large matrix. The above results showed that the introduction of a 1 % of Mn in the Cu/Al_2O_3 catalyst can curb the particle shape and increase its surface area, which are beneficial in improving best catalytic activity for the SCR reaction.

The sufficient amount of metal oxide contraction that promote reduction behavior of the catalyst, which could be originated from the strong interaction between Cu and Mn over the Al_2O_3 support [41]. As for Cat-C, its higher pore volume and BET surface area may be benefited from comparatively smaller mesopores. The particle sizes of Cat-C sample shown by the SEM images were consistent with the BET measurements. The enhanced BET surface areas of Cat-C is also favorable to the adsorption of NO on them, resulted in the significant increase in NO conversion, in turn facilitates the H_2-LPG-SCR reaction.

The low-temperature SCR activity of Cat-C was optimum, revealing that BET surface area was an important decisive factor for catalytic activity. The comparatively high specific surface area exposed to more active sites offered

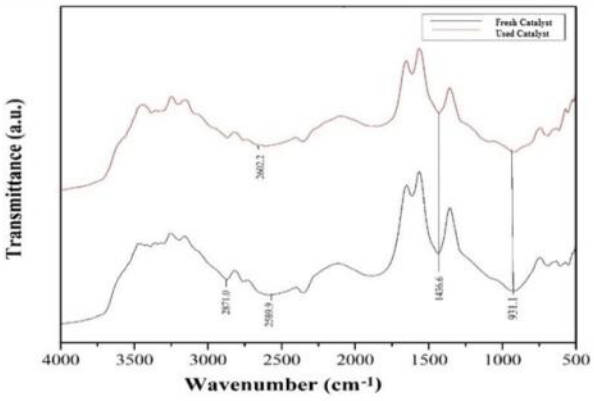

Figure 5. FTIR spectra of fresh and used Cat-C catalysts

Table 3. Transmittance frequency (peak) bond and functional group details on the best Cat-C fresh (t_1) and used (t_2) catalyst using H_2-LPG-SCR of NO

t_1	Interpretations	t_2	Interpretations
2871.0	C–H stretch Alkanes (m)	-	
		2602.4	–C≡C–H: C–H stretch (w) alkynes (terminal)
2589.8	C≡N stretch Nitriles (w)		-
1878.9	-		
1436.6	C–N stretch aliphatic amines (m)	1432.1	C–N stretch aliphatic amines (m)
931.1	O–H bend carboxylic acids (m)	921.0	O–H bend carboxylic acids (m)
-		480.5	-
-		417.9	-

m=medium, w=weak

less diffusional resistance and facilitates the redox process at lower temperatures.

3.2 Catalyst Test for NO reduction

In all catalytic tests, the amount of NO_2 and N_2O in the product stream were found negligible. Therefore, NO was mainly reduced to N_2. All the measurements were taken at steady state by ramping up the temperature.

3.2.1 Performance of catalysts with different reductants

3.2.1.1 Performance of catalysts using NH_3 reductant

NH_3 is a well-established reductant for NO-SCR. The NH_3-SCR performance for NO reduction over different catalysts as shown in Figure 6. It is very clear from the figure that Mn-promoted catalyst showed better performance than Cat-A across the whole temperature range. The NO conversion with respect to temperature showed maxima over all the catalysts. At higher temperature beyond the maximum conversion of NO, reductant started oxidizing directly with oxygen present in air, in place of SCR of NO, so at higher temperature activity of NO conversion decreased. It can be noted down from the figure that the optimum Mn doping in the catalyst was 1.0 mol %, resulting maximum NO conversion to 90 % at 250 °C. Beyond this concentration of 1.0 mol % Mn in the catalyst the conversion decreased in whole range of temperature studied. The catalyst with 1.5 % Mn exhibited lower activity; this may be due to the fact that abundance of Mn does not ensure the increase in catalyst activity as 1 % Mn is the optimum quantity for SCR of NO under the given experimental conditions. It can be noted from the BET characterization that the specific surface area of the catalyst increases with increase in the concentration of Mn upto 1.0 mol%. Further increase in the Mn concentration decreases the surface area of the catalyst, due to agglomeration of particles due to deposition of excess Mn over active sites of Cu.

3.2.1.2 Performance of catalysts using LPG reductant

The activity of all the catalysts was compared using LPG reductant for NO conversion and the results are shown in Figure 7. Cat-C sample showed the highest SCR activity giving 92 % NO conversion at a temperature of 250 ºC. Whereas, the Cat-A catalyst showed 69 % NO reduction at higher temperature of 303 ºC. It is clear from experimental data that Mn doped catalyst have lowered down NO reduction temperature. The above experiments were performed using NH_3 and LPG as reductants under the above mentioned experimental conditions. But, due to low NO reduction activity, hydrogen assisted LPG (H_2-LPG) reductant was used to enhance the catalyst activity.

3.2.1.3 Performance of catalysts using H_2-LPG reductant

The activity of all the catalysts for NO conversion was compared using H_2-LPG reductant and the results are shown in Figure 8. The Cat-C sample exhibited the highest SCR activity showing 95.56 % NO conversion at low temperature of 150 ºC. Whereas, the Cat-A catalyst showed 73 % NO reduction at high temperature of 300 ºC. Figures 6-8 illustrates that the optimum Mn doping was 1.0 mol%. Thus, appropriate composition, textural and morphological characteristics may be the reason for the highest activity of Cat-C.

The catalytic performance of Cat-C showed lower activity at higher temperature due to adsorption sites were used by the reactant in due course of time, which dropped the catalyst activities. The reductants were oxidized at high temperatures and this significantly dropped the NO reduction in case of NH_3 and LPG. The trend differs in H_2-LPG due to synergistic effect of reductants over the better dispersed surface. Whereas, at lower temperature Cat-C exhibited best NO reduction to N_2 due to increased dispersion of smallest particles, which enhanced its BET surface area. In case of Cat-

Table 4. BET surface area and pore parameters of all catalysts

Catalyst	BET surface area ($m^2\ g^{-1}$)	Pore volume ($cm^3\ g^{-1}$)	Pore diameter (nm)
Cat-A	46.14	0.0812	2.87
Cat-B	47.90	0.0847	2.96
Cat-C	50.30	0.0885	3.12
Cat-D	46.85	0.0825	2.91

D, agglomerated particle surface did not support the catalytic reaction, where the adsorption sites are lesser than Cat-C, hindered the catalytic activity.

The experiments were performed to find out the best low temperature NO reduction catalyst. From the experimental results it is clear that Cat-C showed the best results. To elaborate more precisely, we further discussed the effect of reductants over the best catalyst (Cat-C).

3.2.2 Effect of reductants on Cat-C catalyst

To simplify the complexity of all the results, the effects of three reductants (NH_3, LPG, H_2-LPG) for NO conversion over the best selected Cat-C is shown in Figure 9. The characteristic temperature (T_{10}), i.e. 10 % conversion of NO with H_2-LPG was observed at 29 °C, while it was at 26 °C for LPG reductant and 28 °C for NH_3 reductant (Table 5). Similarly, T_{50} was attained at 65 °C for H_2-LPG, 82 °C for LPG and at 75 °C for NH_3. While, T_{max} for NO reduction over Cat-C was shown at 150 °C with 95.56 % NO conversion for H_2-LPG reductant, 92.0 % conversion of NO for LPG at 250 °C and 90 % NO conversion for NH_3 at 250 °C. On the other hand NH_3 reductant showed their NO reduction efficiency at comparatively higher temperatures (205 °C). Hence, the experimental results showed that H_2-LPG is the best reductant in comparison to other two reductants (NH_3 and LPG).

LPG was chosen as a reducing agent as it leads to a strong decrease in Gibbs free energy value of NO reduction to N_2, in addition to its low cost and easy of availability. H_2 addition in LPG not only lowered down the temperature but also improved conversion of NO reduction. It is well documented that hydrogen promotes the redox reactions over Ag/Al_2O_3 catalyst. H_2 played an essential role in the activation of molecular oxygen, as suggested by Richter *et al.* [42] and responsible for the promotion of the steady-state NO reduction [42]. The addition of hydrogen leads to decreased activation energy of the rate-determining step or to a change in the rate-determining step. O_2 activation by hydrogen is relatively rapid and is not involved in the rate-determining step in the H_2-C_3H_8-SCR reaction. This indicates that the hydrogen addition promotes the C_3H_8-SCR reaction through the activation of reductant (C_3H_8) [43,

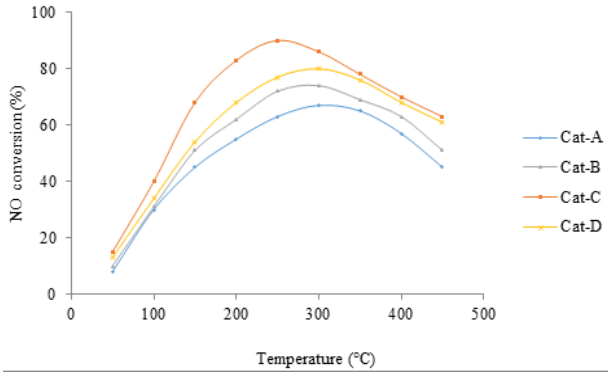

Figure 6. NO reduction performance of all prepared catalysts using NH_3 reductant

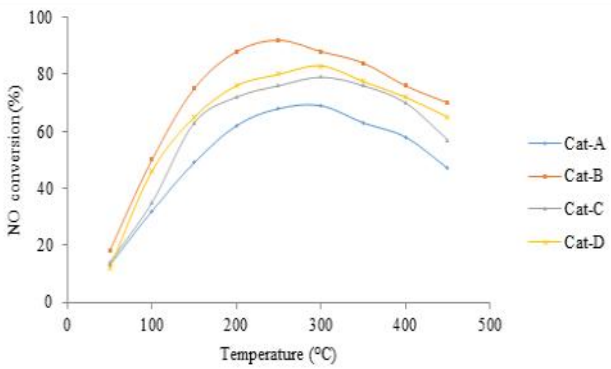

Figure 7. NO reduction performance of all catalysts using LPG reductant

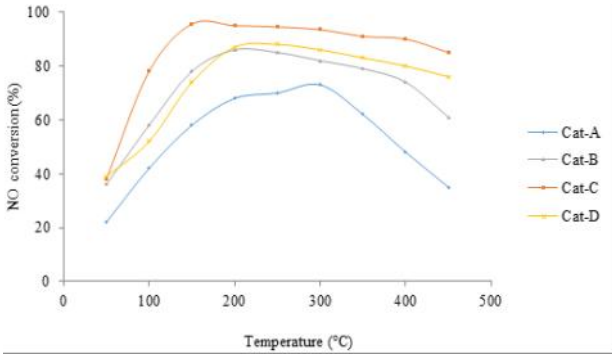

Figure 8. NO reduction performance of all catalysts using H_2-LPG reductant

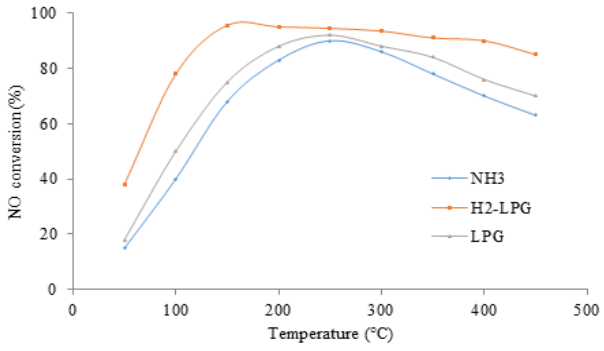

Figure 9. NO conversion with NH_3, LPG and H_2-LPG reductant over the best catalyst (Cat-C)

44]. The addition of hydrogen decreases the activation energy for the reaction of molecular oxygen into reactive oxygen species involved in the oxidative activation of C_3H_8 which is the main constituent of LPG. Thus, the order of reductants according to the performance in the NO-SCR reaction is as follows: H_2-LPG > LPG > NH_3. It is clear from the Figures (6-9) and Table 5 that best low temperature NO reduction is possible with Cat-C catalyst. Thus, the order of catalyst activity followed the same trend for all reductants: Cat-C > Cat-D > Cat-B > Cat-A.

The combination of highly active catalyst and suitable reductants, NO reduction is achievable at low temperature. The histogram plot of NO conversions vs various catalysts and reductants are shown in Figure 10. It can be concluded that the best catalyst and the best reductant for NO reduction are Cat-C and H_2-LPG under the experimental condition of the present study.

3.2.3 LPG conversion

Figure 11 shows LPG conversion over Cat-C with and without H_2 assistance to reduce redundancy at low temperature window. As discussed earlier LPG does not show better NO reduction, so it was not mentioned in the manuscript experimental work. H_2-addition was beneficial showing total LPG conversion at 165 ^oC, i.e. 25 ^oC less than without H_2 addition [23]. Small addition of hydrogen synergistically promoted reduction of NO and being redox reaction simultaneous oxidation of LPG reductant increased. It was found that at 75 ^oC also NO conversion with LPG was (33.7 %) less than H_2-LPG (45.78 %).

Figure 11 shows that the hydrogen addition increases reduction of NO consequently oxidation of LPG increases. As a result of combination of high activity catalyst and apposite reductant, NO conversion is achieved at relatively low temperature. Therefore, it can be concluded that catalyst has the potential to achieve the goal of NOx emission standard from diesel, petrol as well as LPG-fueled vehicles using H_2-LPG-SCR.

3.2.4 Catalyst selectivity

The catalytic activity tests were performed on three catalysts for NO reduction and the

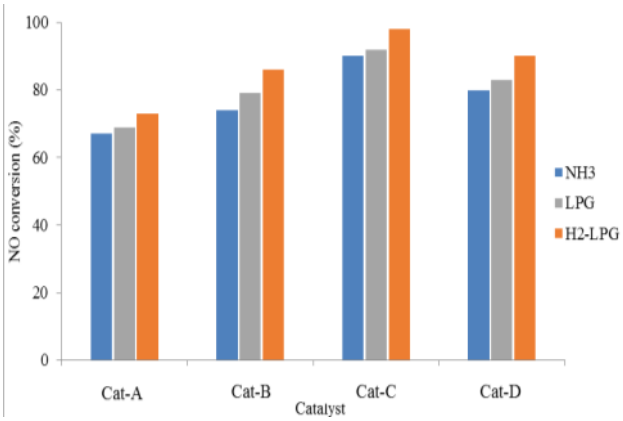

Figure 10. NO conversion performance for NH_3, LPG and H_2-LPG as reductant over different catalysts

Table 5. NO reduction over all catalysts using NH_3, LPG, and H_2-LPG reductants

Catalyst	Reductant	Characteristic Temperature		
		T_{10} (^oC)	T_{50} (^oC)	T_{max} (^oC)
Cat-A	NH_3	32	120	240
	LPG	43	136	286
	H_2-LPG	34	96	200
Cat-B	NH_3	54	131	262
	LPG	48	140	209
	H_2-LPG	37	123	168
Cat-C	NH_3	28	75	205
	LPG	26	68	250
	H_2-LPG	29	65	150
Cat-D	NH_3	43	125	250
	LPG	48	138	303
	H_2-LPG	39	130	245

negligible amount of NO_2 and N_2O were found in the product stream. Therefore, catalyst selectivity was shown in terms of N_2 only. In order to reduce awkwardness in the manuscript here we are presenting the graph of best catalyst selectivity. It is clear from Figure 12 that the trend of best catalyst Cat-C selectivity to N_2 on different reductants is as follows: H_2-LPG > NH_3 > LPG.

3.2.5 Stability test

The stability tests were conducted for Cat-C under the steady state in the same experimental conditions at 150 °C for reduction of NO in a continuous run for 56 h. In the beginning at this temperature 95.56 % NO conversion was achieved. Accelerated ageing starts with 2 h heating at 500 °C under the run duration of 6 h at 150 °C, repeatedly. Practically after 50 h of ageing still no significant deactivation was observed under the same experimental conditions. Figure 13 showed accelerated ageing of Cat-C for NO reduction using H_2-LPG reductant. Thus, practically there is no deactivation of the catalyst occurred in the stability test under the present experimental conditions studied.

4. Conclusions

The enhanced de-NOx performance of Cat-C synthesize by EISA method using PEG-300 template. Among all the catalysts 1.0 mol%-Cu/Al_2O_3 display hydrothermally stable superior H_2 assisted LPG SCR activity with elevated N_2 selectivity over a wide range of temperatures. The catalytic activity attributed to its unique textural characteristics and highly dispersed Mn crystallites which exhibited the redox property with lattice oxygen. The comparatively high specific surface area exposed to more active sites offered less diffusional resistance and facilitates the redox process at lower temperatures. Hydrogen addition promoted reduction of NO consequently increases oxidation of LPG. The results showed that the amount of Mn remarkably influenced the activity of Cu/Al_2O_3. The presence of Mn lowers down NO reduction temperature, consequently Cat-C turn into the most active stable catalyst which can be widely applied in different pollution abatement (ecological safety) applications.

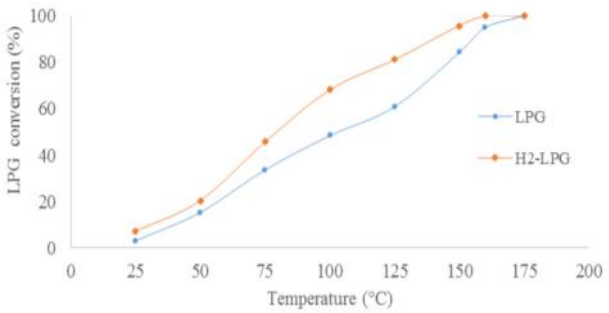

Figure 11. LPG conversion (%) of Cat-C using LPG and H_2-LPG reductants

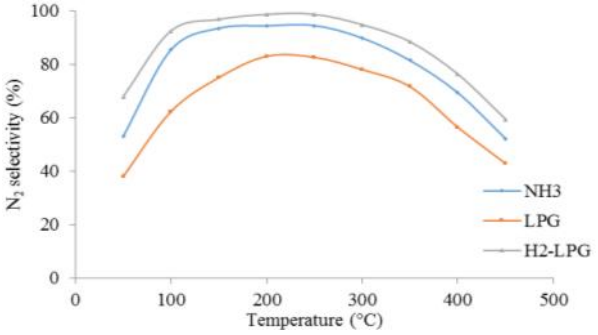

Figure 12. Selectivity of NO to N_2 using different reductants over Cat-C catalyst

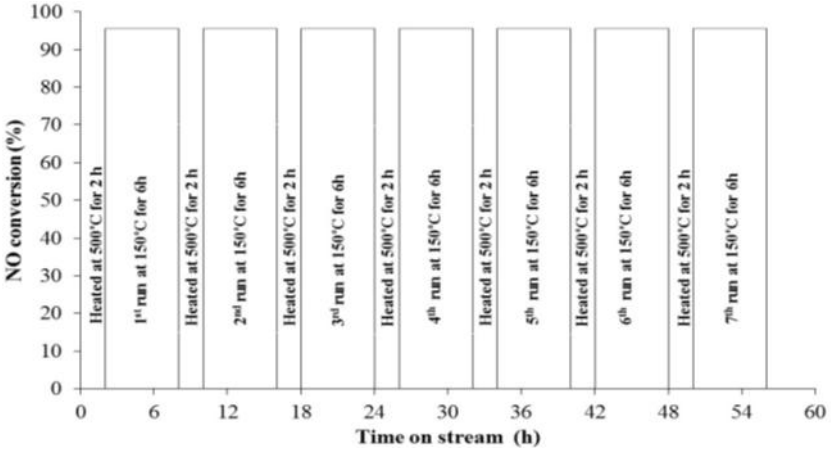

Figure 13. Accelerated ageing of Cat-C for NO reduction

Acknowledgement

The authors are thankful for financial and experimental support from Department of Chemical Engineering & Technology, IIT (BHU) Varanasi.

References

[1] Li, Y., Su, J., Ma J., Yu, F., Chen J., Li R. (2015). Novel Straight Synthesis of Super-Microporous Cu/Al_2O_3 Catalyst with High CH_4-SCR-NO Activity. *Catalysis Communications*, 65: 6-9.

[2] Hu, H., Cai, S., Li, H., Huang, L., Shi, L., Zhang, D. (2015). In Situ DRIFTs Investigation of the Low-Temperature Reaction Mechanism over Mn-Doped Co_3O_4 for the Selective Catalytic Reduction of NOx with NH_3. *Journal of Physical Chemistry C*, 119: 22924-22933.

[3] Chen, Y., Borken-Kleefeld, J. (2016). NOx Emissions from Diesel Passenger Cars Worsen with Age. *Environmental Science & Technology*, 50: 3327-3332.

[4] Janssens, T.V.W., Falsig, H., Lundegaard, L.F., Vennestrøm, P.N.R., Rasmussen, S.B., Moses, P.G., Giordanino, F., Borfecchia, E., Lomachenko, K.A., Lamberti C., Bordiga, S., Godiksen, A., Mossin, S., Beato, P. (2015). A Consistent Reaction Scheme for the Selective Catalytic Reduction of Nitrogen Oxides with Ammonia. *ACS Catalysis*, 5: 2832-2845.

[5] Marberger, A., Elsener, M., Ferri, D., Sagar, A., Schermanz, K., Krocher, O. (2015). Generation of NH_3 Selective Catalytic Reduction Active Catalysts from Decomposition of Supported $FeVO_4$. *ACS Catalysis*, 5: 4180-4188.

[6] Stere, C.E., Adress, W., Burch, R., Chansai, S., Goguet, A., Graham, W.G., De Rosa, F., Palma, V., Hardacre, C. (2014). Ambient Temperature Hydrocarbon Selective Catalytic Reduction of NOx Using Atmospheric Pressure Nonthermal Plasma Activation of a Ag/Al_2O_3 Catalyst. *ACS Catalysis*, 4: 666-673.

[7] Kong, M., Liu, Q., Zhu, B., Yang, J., Li, L., Zhou, Q., Ren, S. (2015). Synergy of KCl and Hg^{el} on Selective Catalytic Reduction of NO with NH_3 over V_2O_5-WO_3/TiO_2 Catalysts. *Chemical Engineering Journal*, 264: 815-823.

[8] Song, Z., Zhang, Q., Ning, P., Liu, X., Zhang, J., Wang, Y., Xu, L., Huang, Z. (2016). Effect of Copper Precursors on the Catalytic Activity of Cu/ZSM-5 Catalysts for Selective Catalytic Reduction of NO by NH_3. *Research on Chemical Intermediates*, 42: 7429-7445.

[9] Pia, M., Grossale, A., Nova, I., Tronconi, E., Jirglova, H., Sobalik, Z. (2012). FTIR In Situ Mechanistic Study of the NH_3 NO/NO_2 "Fast SCR" Reaction over a Commercial Fe-ZSM-5 Catalyst. *Catalysis Today*, 184: 107-114.

[10] Inceesungvorn, B., López-Castro, J., Calvino, J.J., Bernal, S., Meunier, F.C., Hardacre, C., Griffin, K. and Delgado, J.J. (2011). Nano-Structural Investigation of Ag/Al_2O_3 Catalyst for Selective Removal of O_2 with Excess H_2 in the Presence of C_2H_4. *Applied Catalysis A: General*, 391: 187-193.

[11] Kannisto, H., Ingelsten, H.H., Skoglundh, M. (2009). Aspects of the Role of Hydrogen in H_2-Assisted HC-SCR over Ag-Al_2O_3. *Topics in Catalysis*, 52: 1817-1820.

[12] More, P.M., Nguyen, D.L., Granger, P., Dujardin, C., Dongare, M.K., Umbarkar, S.B. (2015). Activation by Pretreatment of Ag-Au/Al_2O_3 Bimetallic Catalyst to Improve Low Temperature HC-SCR of NOx for Lean Burn Engine Exhaust. *Applied Catalysis B: Environmental*, 174-175: 145-156.

[13] Gálvez, M.E., Ascaso, S., Moliner R., Lázaro, M.J. (2013). Me (Cu,Co,V)-KAl_2O_3 Supported Catalysts for the Simultaneous Removal of Soot and Nitrogen Oxides from Diesel Exhausts. *Chemical Engineering Sciences*, 87: 75-90.

[14] Jabłońska, M., Palkovits, R. (2016). Nitrogen Oxide Removal over Hydrotalcite-Derived Mixed Metal Oxides. *Catalysis Science & Technology*, 6: 49-72.

[15] Li, B., Ren, Z., Ma, Z., Huang, X., Liu, F., Zhang, X., Yang, H. (2016). Mechanistic Study of Selective Catalytic Reduction of NO by NH_3 over CuO-CeO_2 in the Presence of SO_2. *Catalysis Science & Technology*, 6: 1719-1725.

[16] Yu, Y., Miao, J., Wang, J., He, C., Chen, J. (2017). Facile Synthesis of $CuSO_4/TiO_2$ Catalysts with Superior Activity and SO_2 Tolerance for NH_3-SCR: Physicochemical Properties and Reaction Mechanism. *Catalysis Science & Technology*, 7: 1590-1601.

[17] Leistner, K., Mihai, O., Wijayanti, K., Kumar, A., Kamasamudram, K., Currier, N.W., Yezerets, A., Olsson, L. (2015). Comparison of Cu/BEA, Cu/SSZ-13 and Cu/SAPO-34 for Ammonia-SCR Reactions. *Catalysis Today*, 258: 49-55.

[18] Turek, W., Plis, A., Costa, P.Da, Krzton, A. (2010) Investigation of Oxide Catalysts Activity in the NOx Neutralisation with Organic Reductants. *Applied Surface Science*, 256: 5572-5575.

[19] Swallow, D. Johnson Matthey Public Limited Company, LONDON. Dec. 27, 2012. Control of Emissions. *US Patent Application no. US 2012/0324867 A1.*

[20] Chmielarz, L., Jabłonska, M. (2015). Advances in Selective Catalytic Oxidation of Ammonia to Dinitrogen: A Review. *RSC Advances*, 5: 43408-43431.

[21] Jeon, J., Lee, J.T., Park, S. (2016). Nitrogen Compounds (NO, NO_2, N_2O, and NH_3) in NOx Emissions from Commercial EURO VI Type Heavy-Duty Diesel Engines with a Urea-Selective Catalytic Reduction System. *Energy & Fuels*, 30: 6828-6934.

[22] Parvulescu, V.I., Grange, P., Delmon, B. (1998). Catalytic Removal of NO. *Catalysis Today*, 46: 233-316.

[23] Kumar, P.A., Reddy, M.P., Ju, L.K., Sook, B.H., Phil, H.H. (2008). Low Temperature Propylene SCR of NO by Copper Alumina Catalyst. *Journal of Molecular Catalysis A Chemical*, 291: 66-74.

[24] Singh P.S., Prasad R., Pandey J. (2015). Development of Green Ag/Al_2O_3 Catalyst by Mechanochemical Method for Low Temperature H_2-LPG-SCR of Lean NOx. *International Journal of Advance Research in Science and Engineering*, 4: 792-801.

[25] Li, Y., Su, J., Ma, J., Yu, F., Chen, J., Li, R. (2015). Novel Straight Synthesis of Super-Microporous Cu/Al_2O_3 Catalyst with High CH_4-SCR-NO Activity. *Catalysis Communications*, 65: 6-9.

[26] Hu, H., Cai, S., Li, H., Huang, L., Shiand, L., Zhang, D. (2015). In Situ DRIFTs Investigation of the Low-Temperature Reaction Mechanism over Mn-Doped Co_3O_4 for the Selective Catalytic Reduction of NOx with NH_3. *Journal of Physical Chemistry C*, 119: 22924-22933.

[27] Lee, T., Bai, H. (2016). Low Temperature Selective Catalytic Reduction of NO x with NH_3 over Mn-based Catalyst: A Review. *AIMS Environmental Science*, 3: 261-289.

[28] Qi, G., Yang, R.T., Chang, R. (2004). MnOx-CeO_2 Mixed Oxides Prepared by Co-precipitation for Selective Catalytic Reduction of NO with NH_3 at Low Temperatures. *Applied Catalysis B: Environmental*, 51: 93-106.

[29] Zhan, S., Qiu, M., Yang, S., Zhu, D., Yua, H., Li,Y. (2014). Facile Preparation of MnO_2 Doped Fe_2O_3 Hollow Nanofibers for Low Temperature SCR of NO with NH_3. *Journal of Materials Chemistry A*, 2: 20486-20493.

[30] Weng, X., Zhang, J., Wu, Z., Liu, Y. (2011). Continuous Hydrothermal Flow Syntheses of Transition Metal Oxide Doped $CexTiO_2$ Nanopowders for Catalytic Oxidation of Toluene. *Catalysis Today*, 175: 386-392.

[31] Lv, G., Bin, F., Song, C., Wang, K., Song, J. (2013). Promoting Effect of Zirconium Doping on Mn/ZSM-5 for the Selective Catalytic Reduction of NO with NH_3. *Fuel*, 107: 217-224.

[32] Jampaiah, D., Ippolito, S.J., Sabri, Y.M., Reddy, B.M., Bhargava, S.K. (2015). Highly Efficient Nanosized Mn and Fe Codoped Ceria-Based Solid Solutions for Elemental Mercury Removal at Low Flue Gas Temperatures. *Catalysis Science and Technology*, 5: 2913-2924.

[33] Meng, D., Zhan, W., Guo, Y., Guo, Y., Wang, L., Lu, G. (2015). A Highly Effective Catalyst of Sm-MnOx for the NH_3-SCR of NOx at Low Temperature: Promotional Role of Sm and Its Catalytic Performance. *ACS Catalysis*, 5: 5973-5983.

[34] Vila, F., López Granados, M., Ojeda, M., Fierro, J.L.G., Mariscal, R. (2012). Glycerol Hydrogenolysis to 1,2-propanediol with Cu/g-Al_2O_3: Effect of the Activation Process. *Catalysis Today*, 187: 122-128.

[35] Li, H., Jiang, X., Huang W., Zheng, X. (2009). Nonthermal-Plasma-Assisted Selective Catalytic Reaction of NO by CH_4 over CuO/TiO_2/ γ-Al_2O_3 Catalyst. *Energy & Fuel*, 23: 2967-2973.

[36] Chen, D., Cen, C., Feng, I., Yao, C., Li, W., Tian, S., Xiong, Y. (2016). Co-catalytic Effect of Al-Cr Pillared Montmorillonite as A New SCR Catalytic Support. *Journal of Chemical Technology & Biotechnology*, 91: 2842-2851.

[37] Zhang, Y., Zheng, Y., Wang, X., Lu, X. (2015). Preparation of Mn–FeOx/CNTs Catalysts by Redox Co-precipitation and Application in Low-Temperature NO Reduction with NH_3. *Catalysis Communications*, 62: 57-61.

[38] Mejía-centeno, I., Castillo, S., Camposeco, R., Marín, J., García, L.A., Fuentes, G.A. (2015). Activity and Selectivity of $V_2O_5/H_2Ti_3O_7$, V_2O_5-$WO_3/H_2Ti_3O_7$ and $Al_2O_3/H_2Ti_3O_7$ Model Catalysts during the SCR-NO with NH_3. *Chemical Engineering Journal*, 264: 873-885.

[39] Zhong, L., Zhong, Q., Cai, W., Zhang, S., Yu, Y., Ou, M., Song, F. (2016). Promotional Effect and Mechanism Study of Nonmetal-Doped $Cr/CexTi_{1-x}O_2$ for NO Oxidation: Tuning O_2 Activation and NO Adsorption Simultaneously. *RSC Advances*, 6: 21056-21066.

[40] Li, Y., Li, Y., Wan, Y., Zhan, S., Tian, Y. (2016). Structure-Performance Relationships of MnO_2 Nanocatalyst for the Low-Temperature SCR Removal of NOx under Ammonia. *RSC Advances*, 6: 54926-54937.

[41] Liu, H., Lin, Y., Ma, Z. (2016). Rh_2O_3/ Mesoporous MOx-Al_2O_3 (M = Mn, Fe, Co, Ni, Cu, Ba) Catalysts: Synthesis, Characterization and Catalytic Applications. *Chinese Journal of Catalysis*, 37: 73-82.

[42] Richter, M., Bentrup, U., Eckelt, R., Schneider, M., Pohl, M., Fricke, R. (2004). The Ef-

fect of Hydrogen on the Selective Catalytic Reduction of NO in Excess Oxygen over Ag/Al_2O_3. *Applied Catalysis B: Environmental*, 51: 261.

[43] Shimizu, K., Shibata, J., Satsuma, A. (2006). Kinetic and In Situ Infrared Studies on SCR of NO with Propane by Silver–Alumina Catalyst: Role of H_2 on O_2 Activation and Retardation of Nitrate Poisoning. *Journal of Catalysis*, 239: 402-409.

[44] Bentrup, U., Richter, M., Fricke R. (2005). Effect of H_2 Admixture on the Adsorption of NO, NO_2 and Propane at Ag/Al_2O_3 Catalyst as Examined by In Situ FTIR. *Applied Catalysis B: Environmental*, 55: 213-220.